Acta Crystallographica Section F
Structural Biology and Crystallization Communications
ISSN 1744-3091

Crystallization of the pneumococcal autolysin LytC: in-house phasing using novel lanthanide complexes

Inmaculada Pérez-Dorado,[a] Reyes Sanles,[a] Ana González,[b] Pedro García,[b,c] José L. García,[b] Martín Martínez-Ripoll[a] and Juan A. Hermoso[a]*

[a]Grupo de Cristalografía Macromolecular y Biología Estructural, Instituto de Química-Física Rocasolano, CSIC, Serrano 119, 28006 Madrid, Spain, [b]Departamento de Microbiología Molecular, Centro de Investigaciones Biológicas, CSIC, Ramiro de Maeztu 9, 28040 Madrid, Spain, and [c]CIBER de Enfermedades Respiratorias (CIBERES), Spain

Correspondence e-mail: xjuan@iqfr.csic.es

Received 13 November 2009
Accepted 15 February 2010

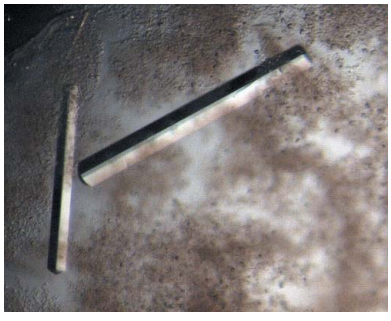

LytC, one of the major autolysins from the human pathogen *Streptococcus pneumoniae*, has been crystallized as needles by the hanging-drop technique using 10%(*w*/*v*) PEG 3350 as precipitant and 10 m*M* HEPES pH 7.5. LytC crystals were quickly soaked in mother liquor containing 2 m*M* of the complex Gd-HPDO3A to produce derivatized crystals ($LytC_{Gd\text{-}HPDO3A}$). Both native LytC and isomorphous $LytC_{Gd\text{-}HPDO3A}$ crystals were flash-cooled in a nitrogen flow at 120 K prior to X-ray data collection using an in-house Enraf–Nonius rotating-anode generator ($\lambda = 1.5418$ Å) and a MAR345 imaging-plate detector. In both cases, good-quality diffraction patterns were obtained at high resolution. $LytC_{Gd\text{-}HPDO3A}$ crystals allowed the collection of a SAD X-ray data set to 2.6 Å resolution indexed in terms of a $P2_1$ monoclinic unit cell with parameters $a = 59.37$, $b = 67.16$, $c = 78.85$ Å, $\beta = 105.69^\circ$. The anomalous Patterson map allowed the identification of one heavy-atom binding site, which was sufficient for the calculation of an interpretable anomalous map at 2.6 Å resolution.

1. Introduction

Most bacterial species examined contain several murein hydrolases that can degrade or remodel the cell wall. In the case of *Streptococcus pneumoniae* up to five enzymes that cleave different covalent bonds in peptidoglycan and (lipo)teichoic acids have been described (López & García, 2004; Eldholm *et al.*, 2009). Nevertheless, only two of them (LytA and LytC) are responsible for causing lysis and death of the cell and consequently are properly named autolysins. LytC is a lysozyme that specifically provokes autolysis of the pneumococci when growing at 303 K (García *et al.*, 1999). LytC belongs to the family of so-called choline-binding proteins (CBPs), which are attached to the bacterial surface through noncovalent interactions with the phosphorylcholine residues that are present in teichoic and lipoteichoic acids (López & García, 2004). Some of these pneumococcal murein hydrolases play important roles in pathogenesis, although their precise function is still unknown (Gosink *et al.*, 2000). *S. pneumoniae* is an important human pathogen with great morbidity and mortality, especially among children and the elderly. In the last two decades, the rise of resistance to penicillin and other antibiotics has triggered a search for new pharmacological targets and the development of innovative weapons. In this regard, the use of cell-wall lytic enzymes from pneumococcal phages such as Cpl-1 or Pal (termed enzybiotics) has yielded promising results to date in the eradication of pneumoccocal infections using animal models (Jado *et al.*, 2003; McCullers *et al.*, 2007). The results presented here constitute an advance towards the structural characterization of LytC, an autolysin and a virulence factor in *S. pneumoniae* (Gosink *et al.*, 2000) and therefore a potential pharmacological target.

A SAD X-ray data set was collected in-house (Cu $K\alpha$ radiation) from the $LytC_{Gd\text{-}HPDO3A}$ derivative. Data processing showed the existence of a good-quality anomalous signal that led to the identification of a single Gd-binding site per asymmetric unit. This single heavy atom was sufficient for the calculation of an initial anomalous map at 2.6 Å resolution, which is currently being used for structural modelling of LytC. Detailed structure determination will help in understanding the function of this enzyme and could open new therapeutic prospects for treating pneumococcal diseases.

2. Experimental procedures

2.1. Protein expression and purification

The mature form of the pneumococcal LytC lysozyme (55 210 Da) was expressed in *Escherichia coli* BL21 (DE3) [pLCC14] strain (García *et al.*, 1999). This cell culture was grown at 310 K with aeration. At an OD_{600} of about 0.4–0.5, protein expression was induced with 40 µ*M* isopropyl *β*-D-1-thiogalactopyranoside and incubation was continued at 293 K for 3 h to minimize the presence of inclusion bodies. Cells were collected by centrifugation, resuspended in 20 m*M* sodium phosphate buffer pH 6.0 and disrupted in a French pressure-cell press (7.6 MPa) at 277 K. The supernatant was loaded onto a DEAE-cellulose column and washed with three volumes of 20 m*M* sodium phosphate buffer pH 6.0 containing 1.5 *M* NaCl. The same buffer containing 2% choline was then added and pure LytC was recovered. Thus, DEAE-cellulose acts to purify CBPS by affinity chromatography, as has been demonstrated previously (Sánchez-Puelles *et al.*, 1992; García *et al.*, 1999). The eluted fractions of the protein with the highest purity were pooled and dialyzed against a buffer containing 20 m*M* Tris–HCl pH 8.0 and 200 m*M* choline using a PD-10 Desalting column from Amersham Pharmacia Biotech. Dialyzed protein samples were concentrated at 277 K using a 10 kDa cutoff protein concentrator (Amicon, YM-10) to the values required for crystallization assays (between 8 and 12 mg ml^{-1}). Under these conditions, LytC precipitated after freezing at 269 K or after several freeze–thaw cycles. Thus, in order to minimize protein degradation, samples were aliquoted and stored at 193 K and those aliquots that were thawed for crystallization trials were maintained at 277 K. The protein concentration was estimated by UV spectrophotometry using a molar absorption coefficient of 196 150 M^{-1} cm^{-1} at 280 nm.

2.2. Crystallization and heavy-atom derivatization

An extensive screening to identify crystallization conditions for LytC was performed using commercial screening kits from Hampton Research (Crystal Screen I, Crystal Screen II and Index). Initial trials were performed by the sitting-drop vapour-diffusion method at 291 K using high-throughput techniques with a Quat-Z 215 robot from Gilson. 250 nl droplets were formed by mixing 125 nl protein solution at 12 mg ml^{-1} and 125 nl precipitant solution. Initial crystals were obtained using condition No. 61 of Index screen, which consisted of 10%(*w*/*v*) PEG 3350, 100 m*M* HEPES pH 7.5 and 200 m*M* proline. Crystallization conditions were subsequently scaled up using the hanging-drop vapour-diffusion method at 291 K; 2 µl droplets (1 µl protein solution and 1 µl precipitant solution) were equilibrated against 500 µl reservoir solution. After scaling, optimization trials yielded a final condition consisting of 2 µl droplets formed by mixing 1 µl protein solution at 8 mg ml^{-1} and 1 µl precipitant solution [10%(*w*/*v*) PEG 3350 and 10 m*M* HEPES pH 7.5]. LytC crystals obtained under these conditions reached maximum dimensions of 0.8 × 0.1 × 0.1 mm in 10–15 d (see Fig. 1). These crystals will be referred to as $LytC_{NATIVE}$. Heavy-atom derivatization was carried out by soaking experiments using the gadolinium complex Gd-HPDO3A (Girard *et al.*, 2003). In these experiments, $LytC_{NATIVE}$ crystals were soaked in 2 µl droplets of mother liquor containing various concentrations of Gd-HPDO3A. High concentrations of the Gd complex (>25 m*M*) and long soaking times generated crystal cracking or a loss of crystal order. In order to minimize this damage, several trials were performed until the optimum conditions were found. These conditions consisted of a 1–2 s soak in mother-liquor solution containing 2 m*M* Gd-HPDO3A. Crystals of LytC derivatized with Gd-HPDO3A will be referred as $LytC_{Gd\text{-}HPDO3A}$.

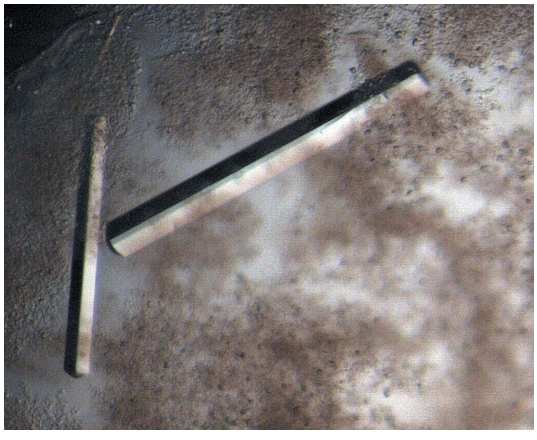

Figure 1
Crystals of wild-type LytC. The crystals grew at 291 K in 10%(*w*/*v*) PEG 3350 and 10 m*M* HEPES pH 7.5.

2.3. X-ray data collection and processing

$LytC_{Gd\text{-}HPDO3A}$ crystals were tested and diffraction data were collected using Cu *Kα* (λ = 1.5418 Å) radiation generated by an in-house Enraf–Nonius FR591 rotating-anode generator operated at 40 kV and 60 mA and equipped with a Helios double-mirror focusing system (Bruker). X-ray photographs were collected using a MAR345 imaging-plate detector. Prior to X-ray data collection, cryoprotected crystals were captured in nylon loops and flash-cooled in a nitrogen flow at 120 K. The cryoprotectant solution used contained 10%(*w*/*v*)

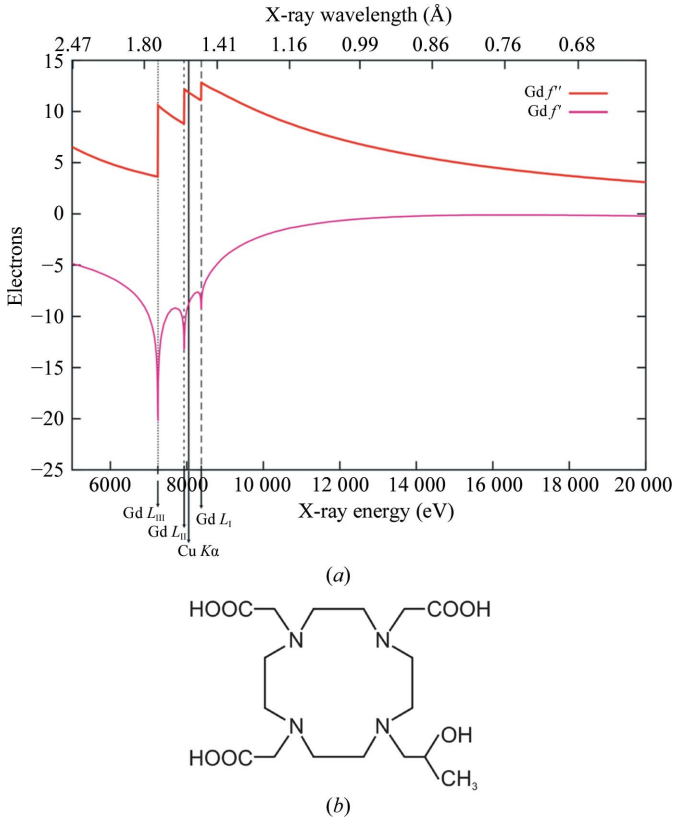

Figure 2
(*a*) Absorption edges for the Gd atom. (*b*) Schematic representation of the HPDO3A macrocycle.

PEG 3350, 10 m*M* HEPES pH 7.5, 20%(*v*/*v*) glycerol and 2 m*M* Gd-HPDO3A. X-ray data were processed and reduced using the programs *MOSFLM* (Leslie, 1992) and *SCALA* from the *CCP*4 package (Collaborative Computational Project, Number 4, 1994).

The large anomalous signal of gadolinium accessible using Cu *Kα* radiation ($f'' = 12$ e$^-$; see Fig. 2*a*) makes Gd extremely useful for phasing using in-house X-ray sources. The use of gadolinium derivatives in the structural resolution of the choline-binding proteins (CBPs) Pce (Lagartera *et al.*, 2005) and CbpF (Molina, González *et al.*, 2009) has previously been reported; the Gd-HPDO3A derivative (Girard *et al.*, 2003) was used in both these cases. This compound consists of a central Gd atom coordinated by a macrocyclic tetraazacyclododecane (Fig. 2*b*). The affinity of Gd-HPDO3A for choline-binding sites means that it should be useful in the phasing of other CBPs (Molina, Stelter *et al.*, 2009). Anomalous signal estimation was performed with the program *SHELX* (Sheldrick, 2008).

3. Results and discussion

Good-quality and high-resolution X-ray diffraction patterns were measured for both LytC$_{\rm NATIVE}$ and the isomorphous LytC$_{\rm Gd\text{-}HPDO3A}$ crystals using Cu *Kα* radiation generated by an in-house rotating-anode generator. The best LytC$_{\rm Gd\text{-}HPDO3A}$ crystal allowed us to collect a SAD X-ray data set to 2.6 Å resolution (Fig. 3). Automatic indexing of the diffraction images of this derivative identified the space group as primitive monoclinic (*P*2 or *P*2$_1$), with unit-cell parameters $a = 59.37$, $b = 67.16$, $c = 78.85$ Å, $\beta = 105.69^\circ$. Integrating and scaling the diffraction data in space group *P*2 yielded an overall $R_{\rm merge}$ value of 0.11 (Table 1), confirming the space-group symmetry. Systematic absences along 0*k*0 of $k = 2n$ indicated the space group to be *P*2$_1$. Calculation of the Matthews coefficient revealed a solvent content of 55% for a single molecule in the asymmetric unit ($V_{\rm M} = 2.74$ Å^3 Da^{-1}; Matthews, 1968). An anomalous Patterson map calculated for the entire X-ray data set displayed one single and clear peak of 6.5σ, indicating the presence of a single Gd atom in the asymmetric unit (two Gd atoms per unit cell). Analysis of the values obtained from *SHELXC* (Sheldrick, 2008) revealed anomalous signal to 3.3 Å resolution. Structural modelling and refinement is currently in progress.

Table 1
Data-collection statistics for LytC crystals.

Values in parentheses are for the highest resolution shell.

Crystal data	
Space group	*P*2$_1$
Unit-cell parameters	
a (Å)	59.37
b (Å)	67.16
c (Å)	78.85
β (°)	105.69
Data collection	
Wavelength (Å)	1.5418
Temperature (K)	120
Resolution (Å)	30.57–2.57 (2.71–2.57)
Total No. of reflections†	124908
No. of unique reflections†	18467
Centric	1038 (24)
Acentric	17429 (218)
Redundancy†	6.7 (6.7)
Anomalous redundancy†	3.5 (3.4)
Completeness† (%)	99.4 (99.0)
Anomalous completeness† (%)	99.3 (98.7)
$I/\sigma(I)$†	14.8 (3.8)
$R_{\rm merge}$†‡	0.12 (0.49)
$R_{\rm ano}$†	0.07 (0.22)

† Parameters provided by *SCALA*. ‡ $R_{\rm merge} = \sum_{hkl}\sum_i |I_i(hkl) - \langle I(hkl)\rangle|/\sum_{hkl}\sum_i I_i(hkl)$.

In summary, in-house SAD experiments have allowed us to calculate initial anomalous maps using a single Gd atom per polypeptide chain. These results reflect not only the utility of these lanthanide derivatives for in-house macromolecular phasing, but also the excellent quality of the anomalous signal obtained, which enabled us to phase a 55 210 Da protein using a single heavy atom.

The authors thank Bracco Imaging (Milan) for kindly providing a sample of Gd-HPDO3A. This work was supported by grants from the Spanish Ministry of Science and Technology (BFU2008-01711, SAF2006-00390 and the Factoría de Cristalización from the CONSOLIDER-INGENIO 2010 program), EU-CP223111 (CAREPNEUMO, European Union). CIBER de Enfermedades Respiratorias is an initiative of Spanish Instituto de Salud Carlos III. IP-D and SR were granted I3P-CSIC and FPI fellowships, respectively.

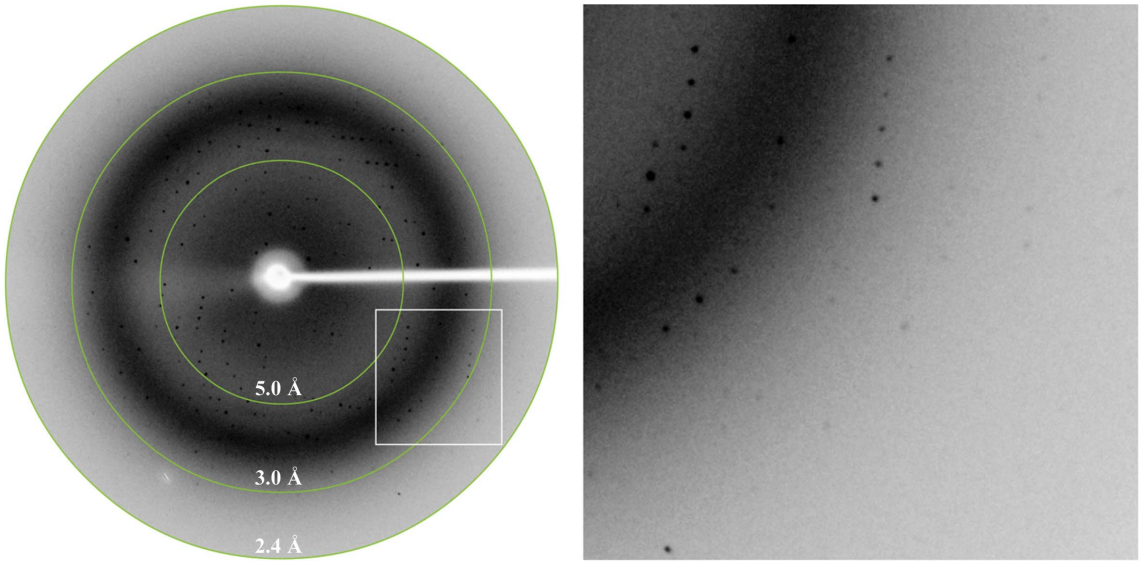

Figure 3
1° oscillation image of a LytC$_{\rm Gd\text{-}HPDO3A}$ crystal.

References

Collaborative Computational Project, Number 4 (1994). *Acta Cryst.* D**50**, 760–763.

Eldholm, V., Johnsborg, O., Haugen, K., Ohnstad, H. S. & Havarstein, L. S. (2009). *Microbiology*, **155**, 2223–2234.

García, P., González, M. P., García, E., García, J. L. & López, R. (1999). *Mol. Microbiol.* **33**, 128–138.

Girard, É., Stelter, M., Vicat, J. & Kahn, R. (2003). *Acta Cryst.* D**59**, 1914–1922.

Gosink, K. K., Mann, E. R., Guglielmo, C., Tuomanen, E. I. & Masure, H. R. (2000). *Infect. Immun.* **68**, 5690–5695.

Jado, I., López, R., García, E., Fenoll, A., Casal, J. & García, P. (2003). *J. Antimicrob. Chemother.* **52**, 967–973.

Lagartera, L., González, A., Stelter, M., García, P., Kahn, R., Menéndez, M. & Hermoso, J. A. (2005). *Acta Cryst.* F**61**, 221–224.

Leslie, A. G. W. (1992). *Crystallographic Computing 5: From Chemistry to Biology*, edited by D. Moras, A. D. Podjarny & J. C. Thierry, pp. 39–50. Oxford University Press.

López, R. & García, E. (2004). *FEMS Microbiol. Rev.* **28**, 553–580.

Matthews, B. W. (1968). *J. Mol. Biol.* **33**, 491–497.

McCullers, J. A., Karlstrom, A., Iverson, A. R., Loeffler, J. M. & Fischetti, V. A. (2007). *PLoS Pathog.* **3**, e28.

Molina, R., González, A., Stelter, M., Pérez-Dorado, I., Kahn, R., Morales, M., Moscoso, M., Campuzano, S., Campillo, N. E., Mobashery, S., García, J. L., García, P. & Hermoso, J. A. (2009). *EMBO Rep.* **10**, 246–251.

Molina, R., Stelter, M., Kahn, R. & Hermoso, J. A. (2009). *Acta Cryst.* D**65**, 823–831.

Sánchez-Puelles, J. M., Sanz, J. M., García, J. L. & García, E. (1992). *Eur. J. Biochem.* **203**, 153–159.

Sheldrick, G. M. (2008). *Acta Cryst.* A**64**, 112–122.